Increased Neural Strength and Reliability to Audiovisual Stimuli at the Boundary of Peripersonal Space

Jean-Paul Noel[1], Andrea Serino[2,3], and Mark T. Wallace[1,4]

Abstract

■ The actionable space surrounding the body, referred to as peripersonal space (PPS), has been the subject of significant interest of late within the broader framework of embodied cognition. Neurophysiological and neuroimaging studies have shown the representation of PPS to be built from visuotactile and audiotactile neurons within a frontoparietal network and whose activity is modulated by the presence of stimuli in proximity to the body. In contrast to single-unit and fMRI studies, an area of inquiry that has received little attention is the EEG characterization associated with PPS processing. Furthermore, although PPS is encoded by multisensory neurons, to date, there has been no EEG study systematically examining neural responses to unisensory and multisensory stimuli, as these are presented outside, near, and within the boundary of PPS. Similarly, it remains poorly understood whether multisensory integration is generally more likely at certain spatial locations (e.g., near the body) or whether the cross-modal tactile facilitation that occurs within PPS is simply due to a reduction in the distance between sensory stimuli when close to the body and in line with the spatial principle of multisensory integration. In the current study, to examine the neural dynamics of multisensory processing within and beyond the PPS boundary, we present auditory, visual, and audiovisual stimuli at various distances relative to participants' reaching limit—an approximation of PPS—while recording continuous high-density EEG. We question whether multisensory (vs. unisensory) processing varies as a function of stimulus–observer distance. Results demonstrate a significant increase of global field power (i.e., overall strength of response across the entire electrode montage) for stimuli presented at the PPS boundary—an increase that is largest under multisensory (i.e., audiovisual) conditions. Source localization of the major contributors to this global field power difference suggests neural generators in the intraparietal sulcus and insular cortex, hubs for visuotactile and audiotactile PPS processing. Furthermore, when neural dynamics are examined in more detail, changes in the reliability of evoked potentials in centroparietal electrodes are predictive on a subject-by-subject basis of the later changes in estimated current strength at the intraparietal sulcus linked to stimulus proximity to the PPS boundary. Together, these results provide a previously unrealized view into the neural dynamics and temporal code associated with the encoding of nontactile multisensory around the PPS boundary. ■

INTRODUCTION

Many of the interactions between a living organism and their environment happen within the peripersonal space (PPS; di Pellegrino, Làdavas, & Farnè, 1997; Rizzolatti, Fadiga, Fogassi, & Gallese, 1997; Rizzolatti, Scandolara, Matelli, & Gentilucci, 1981)—the actionable space immediately adjacent to and surrounding one's body. In nonhuman primates, the neural instantiation of PPS has been linked to a multisensory-motor frontoparietal network (Graziano, Hu, & Gross, 1997; Fogassi et al., 1996). Neurons within the intraparietal sulcus (IPS) and the ventral premotor cortex (vPM) respond both to somatosensory stimuli presented on the body, as well as to visual (Schlack et al., 2005; Duhamel et al., 1998; Duhamel, Bremmer, Ben Hamed, & Graf, 1997) and/or auditory (Schlack et al., 2005; Graziano, Reiss, & Gross, 1999)

stimuli presented near (∼30–45 cm), but not far from, the body. Furthermore, the receptive fields of neurons within the PPS network are anchored on the body (Graziano et al., 1997, 1999; Duhamel et al., 1998) and are both highly plastic and dynamic, expanding and contracting based on interactions with the environment—such as tool use (Iriki et al., 1996; see Berti & Frassinetti, 2000, for a similar effect in humans)—and rapidly adapting as a function of the properties of external stimuli—such as the velocity of approaching stimuli (Fogassi et al., 1996; see Noel, Blanke, Magosso, & Serino, 2018). The representation of PPS is thus conceived as a body–environment interface that is crucial in defensive or avoidance behaviors (Graziano & Cooke, 2006), as well as in sensorimotor affordances (Serino et al., 2017; de Vignemont & Iannetti, 2015).

An analogous neural system has been demonstrated in humans, first via work in neuropsychology (Farnè & Ladavas, 2000, 2002; Làdavas, 2002; Farnè, Pavani, Meneghello, & Ladavas, 2000; Làdavas, di Pellegrino, Farnè, & Zeloni, 1998; di Pellegrino et al., 1997) and then via

[1]Vanderbilt University, Nashville, TN, [2]University of Lausanne, [3]Ecole Polytechnique Federale de Lausanne, [4]Vanderbilt University Medical Center, Nashville, TN

psychophysics (Noel, Park, et al., 2018; Pfeiffer, Noel, Serino, & Blanke, 2018; Salomon et al., 2017; Serino et al., 2015, 2017; Galli, Noel, Canzoneri, Blanke, & Serino, 2015; Noel, Grivaz, et al., 2015; Noel, Pfeiffer, Blanke, & Serino, 2015; Occelli, Spence, & Zampini, 2011; Macaluso & Maravita, 2010; Zampini, Torresan, Spence, & Murray, 2007; Pavani & Castiello, 2004; Spence, Pavani, & Driver, 2004; Spence, Pavani, Maravita, & Holmes, 2004; Maravita, Spence, & Driver, 2003) and neuroimaging (Brozzoli, Gentile, & Ehrsson, 2012; Brozzoli, Gentile, Petkova, & Ehrsson, 2011; Gentile, Petkova, & Ehrsson, 2011; Makin, Holmes, & Zohary, 2007) studies. Neuroimaging studies have demonstrated that, as in nonhuman primates, a frontoparietal network made up of the IPS and vPM encodes for the space near the body (Brozzoli et al., 2011, 2012; Makin et al., 2007; Bremmer et al., 2001, see Grivaz et al., 2017, for a recent meta-analysis). However, almost all of the work to date on the neural representation of PPS has been carried out using fMRI (for notable exceptions utilizing EEG, see Sambo & Foster, 2009; Valdés-Conroy, Sebastián, Hinojosa, Román, & Santaniello, 2014; for a recent ECOG study, see Bernasconi et al., 2018), a method with excellent spatial but poor temporal resolution. Hence, questions surrounding the neural dynamics associated with PPS encoding, as well as bridging between the evidence at the level of the single neuron and more global measures of neural activity, remain underexplored. The current work is centered around these neural dynamics and designed to address whether the recruitment of PPS neurons in IPS and vPM results in notable alteration of the EEG signal. Building on this, at what latencies is space-dependent multisensory processing apparent (see Molholm et al., 2002; Foxe et al., 2000, for evidence of multisensory integration occurring at surprisingly early latencies; see Ghazanfar & Schroeder, 2006, for a review)? Finally, does the putative activity of IPS and vPM PPS neurons when stimuli are presented in near space result in a categorically distinct neural network being recruited (as indexed via EEG) than when stimuli are presented far?

Although the neurons encoding for PPS respond to tactile, visual, and auditory stimulation (Schlack et al., 2005; Graziano et al., 1999; Duhamel et al., 1997), to the best of our knowledge, no EEG study to date has examined the interplay between multisensory encoding and the human PPS representation (see Avillac et al., 2007, for a characterization of the multisensory properties of PPS neurons in the nonhuman primate). Perhaps more importantly, although the PPS is widely taken to enhance the detection of multisensory stimuli (e.g., Kandula, van der Stoep, Hofman, & Dijkerman, 2017; Teramoto, Honda, Furuta, & Sekiyama, 2017; de Haan, Smit, van der Stigchel, & Dijkerman, 2016), it is unclear whether the PPS is a zone of privileged multisensory processing beyond its well-established role in somatosensory processing. That is, the vast majority of psychophysical studies of PPS have examined multisensory associations in which an exteroceptive sensory modality, for example, audition (Pfeiffer et al., 2018; Noel, Pfeiffer, et al., 2015) or vision (Noel, Park, et al., 2018; Salomon et al., 2017), is paired with tactile target detection. Results routinely demonstrate facilitated tactile detection when auditory or visual stimuli are presented near as opposed to far from the body, and this evidence is taken to index a PPS representation. However, as the exteroceptive stimulation is brought closer to participants, the spatial principle of multisensory integration (Murray & Wallace, 2012; Meredith & Stein, 1996) comes into play. In this principle, paired unisensory signals are integrated and result in the greatest multisensory gain when the respective stimuli are in spatial proximity to one another. Thus, in traditional PPS studies, approaching stimuli have the dual effect of both altering observer–stimuli distance (e.g., PPS), as well as increasing the proximity of the stimuli to one another (Van der Stoep, Serino, Farnè, Di Luca, & Spence, 2016). An underutilized technique to avoid this confound is to study the impact of stimuli–observer distance on nontactile multisensory pairings (given that tactile receptive fields are by definition on the body). Interestingly, recent psychophysical evidence has suggested that the distance at which audiovisual stimuli are presented—within or beyond the PPS—impacts the degree of multisensory gain (Noel, Modi, Wallace, & Van der Stoep, 2018; Van der Stoep, Van der Stigchel, Nijboer, & Van der Smagt, 2016; Van der Stoep, Nijboer, Van der Stigchel, & Spence, 2015) and binding (Noel, Modi, et al., 2018; Noel, Lukowska, Wallace, & Serino, 2016; Corveleyn, Lopez-Moliner, & Coello, 2015) observed. Similarly, IPS and vPM have been shown to encode for not only visuotactile and audiotactile pairings but also for the pairing of audiovisual stimuli (Werner & Noppeney, 2010; Saito et al., 2005).

In the current study, we record high-density EEG signals from human subjects to study the neural dynamics of the encoding of audiovisual stimuli at different distances from the body and, in particular, within, near, and outside the boundary of PPS. Auditory, visual, and audiovisual stimuli are presented at different distances to ascertain whether observer–stimulus distance affects unisensory and multisensory processing differently. In addition to examining global measures of neural response strength and topography under different sensory stimulation conditions and at different distances relative to the subject and PPS boundary, we were also interested in indexing the variability of ERPs. The analytical focus on variability was motivated by computational models and neurophysiological studies that suggest reduced variability under multisensory conditions (Fetsch et al., 2013; Knill & Pouget, 2004; Ernst & Banks, 2002) as well as by the pivotal role played by neural variability in the plasticity of sensorimotor representations (Mandelblat-Cerf, Paz, & Vaadia, 2009; Faisal, Selen, & Wolpert, 2008; Rokni, Richardson, Bizzi, & Seung, 2007; Churchland, Yu, Ryu, Santhanam, & Shenoy, 2006) and of the PPS

representation, in particular. Indeed, although Ferri et al. (2015) recently suggested that, whereas mean firing rates index the transition into the PPS in nonhuman primate single-unit electrophysiology (e.g., Graziano et al., 1997, 1999; Fogassi et al., 1996), in human fMRI, it is the intertrial variability in the premotor cortex BOLD signal in response to audiotactile stimulation that covaries with PPS size (Ferri et al., 2015). In turn, here we were interested in examining whether EEG intertrial variability was related to multisensory processing within, at the boundary, and beyond the PPS.

By implementing the above-described experimental design—in particular the use of audiovisual stimuli that are always colocalized in space—two opposing views can be tested. If audiovisual stimuli evoke differential neural responses in near versus far space, then multisensory integration is modulated by distance beyond that predicted based on the relative distance/timing of the component unisensory stimuli. If such results are not found, then enhanced audiotactile (Pfeiffer et al., 2018; Noel, Pfeiffer, et al., 2015) and visuotactile (Noel, Park, et al., 2018; Salomon et al., 2017) responses in near space are likely a result of the spatial principle of multisensory integration (Murray & Wallace, 2012; Meredith & Stein, 1996).

METHODS

Participants

Twenty (mean age = 24.6 ± 3.9, range = 18.3–32.3, 11 women) right-handed students from Vanderbilt University took part in this experiment. The lack of prior studies employing a multisensory oddball detection task as a function of distance (see below) in conjunction with electrical neuroimaging (Grave de Peralta Menendez, Murray, Michel, Martuzzi, & Gonzalez Andino, 2004) precluded us from estimating putative effect sizes and thus from power calculation. However, a sample of 20 participants is well in line with previous EEG studies of PPS (Sambo & Foster, 2009, $n = 15$; Valdés-Conroy et al., 2014, $n = 22$). The data from three participants were discarded due to large degrees of electrical noise or technical problems; hence, the final data set consisted of 17 participants (mean age = 23.9 ± 3.7, range = 18.3–32.3, 10 women; Sambo & Foster, 2009, excluded three participants; Valdés-Conroy et al., 2014, excluded two participants due to noise). All participants reported normal hearing and had normal or corrected-to-normal vision. All participants gave their written informed consent to take part in this study; the protocols for which were approved by Vanderbilt University Medical Center's Institutional Review Board.

Materials and Apparatus

Visual and auditory stimuli were driven via a microcontroller (SparkFun Electronics, Redboard) and direct serial port communication under the control of purpose written MATLAB (MathWorks) and Arduino scripts. Visual stimuli were a flash of light presented by means of a red LED (3 mm diameter, 640 nm wavelength), whereas auditory stimuli consisted of a 4-kHz tone, presented via a Piezo Buzzer (12 mm diameter, 9.7 mm tall, 60 dB(A), 3 V rectangular wave). These stimuli were 10 msec in duration (square-wave, onset and offset <1 msec, as measured via oscilloscope). The LED and Piezo Buzzer were mounted into a 5 cm × 3 cm × 1 cm opaque rectangular box, thus forming a single audiovisual object (see Figure 1A; also see Noel et al., 2016). Audiovisual stimuli consisted of the synchronous presentation of the audio and visual stimuli described above. In addition, there were audio, visual, and audiovisual oddball trials, in which stimuli were 100 msec (vs. 10 msec in the standard trial) in duration.

Procedure and Experimental Design

Participants were fitted with a 128-electrode EGI Netstation EEG cap and seated in a dimly lit and sound controller room (Noel, Simon, et al., 2018; Simon, Noel, & Wallace, 2017). Participants completed a total of eight blocks of auditory, visual, and audiovisual oddball detection task to keep them attending to the stimuli presented. In the oddball paradigm, participants were required to press a button for trials in which the stimuli are of long duration (100 msec; these trials were not used for EEG analysis) and to withhold from button presses for stimuli of short duration (10 msec; which were of interest for EEG analysis). Visual, auditory, and audiovisual stimuli were presented at each of four different distances. These distances were personalized for each participant. Once seated, participants were asked to reach out as far as possible on the table placed in front of them with their right arm/hand. This distance was marked (at the tip of their index finger), and on different blocks, the audiovisual apparatus was placed either 15 cm or 5 cm, within or outside their reaching boundary (see Figure 1A). During the experiment itself, participants kept their hands on their lap, where response buttons were placed. This boundary is taken to roughly index the participant's PPS (Patané, Farnè, & Frassinetti, 2017; Patané, Iachini, Farnè, & Frassinetti, 2016; Bourgeois, Farne, & Coello, 2014; Valdés-Conroy et al., 2014). The reach length of subjects participating in the study was not measured, but the average functional grip reach for adults in the geographic region where the study was conducted is between 68 cm (women) and 74 cm (men; Fryar, Gu, Ogden, & Flegal, 2016; Gordon et al., 1989). Thus, Distance 1 approximately corresponded to an observer–stimulus distance of 53–59 cm (on average), which is outside the estimated size of perihand space (~45 cm; Serino et al., 2015), but within the peritrunk space (~72 cm; Serino et al., 2015). Two blocks were completed for each of the four different stimuli distances, resulting in a total of eight blocks, each block consisting of 330 trials: 100 standard (i.e., 10 msec) audio, visual, and audiovisual trials and 10 oddball (i.e., 100 msec)

audio, visual, and audiovisual trials (thus, ~9% of trials were oddballs). Trial order was randomized within each block, and block order (i.e., distance at which stimuli were presented) was counterbalanced across participants. ISI was set between 850 and 1400 msec (uniform distribution), and total duration of the experiment was approximately 2.5 hr.

EEG Acquisition and Preprocessing

High-density continuous EEG was recorded from 128 electrodes with a sampling rate of 1000 Hz (Net Amps 200 amplifier, Hydrocel GSN 128 EEG cap, EGI Systems, Inc.) and referenced to the vertex. Electrode impedances were maintained below 50 kΩ throughout the recording procedure and were reassessed at the end of every other block. Data were acquired with Netstation 5.1.2 running on a Macintosh computer and online high-pass filtered at 0.1 Hz.

Offline, data were exported to EEGLAB (Delorme & Makeig, 2004), band-pass filtered (zero phase, eighth-order Butterworth filter) between 0.1 and 40 Hz, notch filtered at 60 Hz, and epoched from −250 to 500 msec after target onset. EEG epochs containing movement, eye blinks, or other noise transients and artifacts were removed by visual inspection (Noel, Simon, et al., 2018; Simon et al., 2017; Valdés-Conroy et al., 2014; Murray, Brunet, & Michel, 2008). Subsequently, epochs were sorted vis-à-vis sensory condition (audio, visual, or audiovisual) and distance—EEG of oddball trials was not analyzed. After epoch rejection, on average every condition (3 sensory modalities: audio, visual, and audiovisual × 4 distances) had 172.6 ± 32.9 trials (average epoch rejection = 13.7%; no difference between conditions; all ps > .23). Bad channels were then removed (1.2 electrodes on average, 0.94%), data were rereferenced to the average, baseline corrected to the prestimulus period, and bad channels were reconstructed using a spherical spline interpolation (Perrin, Pernier, Bertrand, Giard, & Echallier, 1987). To account for the inherent multiple comparisons problem in EEG, we set alpha at <.01 for at least 10 consecutive time points (Guthrie & Buchwald, 1991).

Sensor Space Analyses

In a first pass, global electric field strength and topographical organization of evoked responses were quantified. To measure the neural strength of evoked re-sponses while attempting to reduce the inherent high dimensionality of EEG data (leading to false-positives), we derived the global field power (GFP; Lehmann & Skrandies, 1980) for each sensory modality condition and distance of presentation. This measure is equivalent to the spatial standard deviation of the trial-averaged voltage values across the entire electrode montage at a given time point and represents a reference- and topographic-independent measure of evoked potential strength. The utilization of this method reduces the dimensionality of

the data by coalescing 128 electrodes (and thus time courses) into a unique one. GFP was calculated and statistically contrasted across conditions on a millisecond-by-millisecond basis (see Results section).

We equally examined differences in the topography of electrical fields generated by the different experimental conditions, an orthogonal measure to GFP and independent of response strength. Changes in topography forcibly follow from changes in the configuration of the underlying active electric dipoles (Lehmann, 1987; although the contrary is not necessarily true), and thus, we performed topographical analyses to index if and when experimental conditions activated distinct sets of brain networks. To test the topography of evoked potentials as a function of sensory modality and distance independently of their strength, we used a Global Dissimilarity (DISS) measure (Lehmann & Skrandies, 1980). DISS is equivalent to the root-square-mean difference between the potentials measured at each electrode for the different conditions, normalized by the instantaneous GFP (L2-norm, in this case). An initial time-wise 3 (sensory modalities) × 4 (distances) topographic ANOVA on DISS values was performed to identify statistical differences between neural generators configuration for the distinct sensory modalities and as a function of distance. This analysis is based on a nonparametric randomization procedure (5000 randomizations per time point) as implemented in the RAGU software (Koenig et al., 2011).

Lastly, we were particularly interested in indexing variability of the evoked neural response, as previous studies have demonstrated that the intersubject variability in PPS size may be accounted for by neural variability in PPS areas (Ferri et al., 2015), and a reduction in variability is a hallmark of multisensory processes (Fetsch et al., 2013; Ernst & Banks, 2002). To do so, thus, we first assured that, for every condition and participant, we had an equal amount of trials. The 100 repetitions with a GFP most similar to the condition's mean GFP were selected for each participant. This number of repetitions was selected as it was the maximum common denominator of good trials for all participants and conditions. Then, over electrodes that demonstrated a significant alteration in neural strength as a function of distance (see GFP results), mean intertrial variance was calculated at each time point. Furthermore, to control for the potential impact of outlier trials, we additionally calculated median absolute deviation, a robust measure of variability (Leys, Ley, Klein, Bernard, & Licata, 2013; see Milne, 2011, for a similar approach). Results were unchanged whether indexing intertrial variance or median absolute deviation, and thus, here we present the former analysis as it is more intuitive. As a control, we also performed this variance analysis on electrodes not demonstrating a strength modulation as a function of sensory modality and distance; this analysis is presented in the Appendix (Figure A1) and demonstrates no difference in ERP reliability as a function of distance and sensory modality.

Source Estimation

For conditions and time periods demonstrating a significant modulation in global strength as a function of presentation location (i.e., near PPS boundary vs. far from PPS boundary), we estimated in the brain the localization of the electrical activity reflected at the sensor level. To do so, for each participant and electrode, we first averaged voltage across the entire epoch of significance (between 323 and 371 msec for GFP), thereby enhancing the signal-to-noise ratio of the data from each participant. Then, ERP data were spatially down-sampled and affine-transformed to a common 111-channel montage. Subsequently, we used a distributed linear inverse solution applying the LAURA regularization approach, which comprises homogenous regression coefficients in all directions within the whole solution space, as well as biophysical laws as constraints (Grave de Peralta Menendez et al., 2004; Grave de Peralta Menendez, Gonzalez Andino, Lantz, Michel, & Landis, 2001; see also Michel et al., 2004, for a review). LAURA projects electrode-level recordings into brain space by using a realistic head model, and the solution space included 4024 nodes, selected from a 6 × 6 × 6 mm grid equally distributed within the gray matter of the Montreal Neurological Institute's average brain (Martuzzi et al., 2009; Gonzalez Andino, Murray, Foxe, & de Peralta Menendez, 2005; Grave de Peralta Menendez et al., 2004; Michel et al., 2004). Hence, applying the LAURA algorithm to averaged voltages during the GFP significance period results in inferred current estimates (i.e., A/mm^2) in the brain during the time period of GFP significance.

Regarding statistical analysis within the source space, data were first submitted to a paired t test (near PPS boundary vs. far from PPS boundary) and then corrected for multiple comparisons via two criteria (Thelen, Cappe,

& Murray, 2012). First, a spatial extent criterion of at least 17 contiguous significant nodes was applied (see Knebel & Murray, 2012; Cappe, Thut, Romei, & Murray, 2010; De Lucia, Clarke, & Murray, 2010, for a similar spatial criterion). This spatial criterion was determined using the AlphaSim program (available at http://afni.nimh.nih.gov) while assuming a spatial smoothing of 6 mm FWHM. This criterion indicates that there is a 3.54% probability of a cluster of at least 17 contiguous nodes, which is equivalent to a node-level p value of $p \leq .0002$. Second, and because distributed source models yield nonzero values in all solution points, it is conceivable that statistical effects may be obtained in nodes that are weakly responsive (i.e., have current density values that are close to zero or alternatively well below the mean across the entire set of nodes in the brain volume). To minimize the contribution of such "ghost" sources, we removed all nodes with current density values less than or equal to 2 SDs below the volume's mean within each condition. In this way, we sought to limit statistical effects to nodes that could reasonably be described as active sources. The results of the source estimations were rendered on the Montreal Neurological Institute's average brain with the Talairach and Tournoux (1988) coordinates.

RESULTS
Behavior

As expected, overall participants exhibited a very modest number of false alarms ($M = 3.2\%$, $SEM = 2.8\%$), and a 3 (sensory modalities) × 4 (distances) repeated-measures ANOVA on accuracy revealed no significant main effect (all $Fs > 1.35$, all $ps > .21$), nor an interaction between these variables, $F(6, 96) = 0.77$, $p = .59$. Regarding RTs, however, as illustrated in Figure 1B, a 3 (sensory
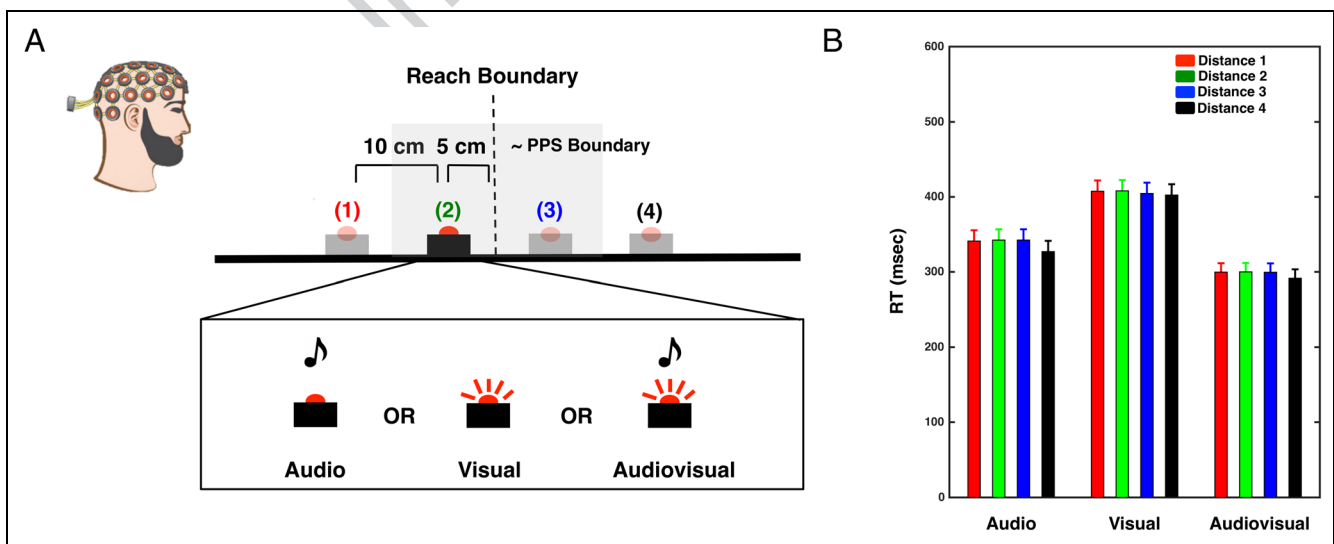

Figure 1. Experimental design and behavioral results. (A) Participants viewed audio, visual, or audiovisual stimuli presented either 15 cm (Distance 1, red) or 5 cm (Distance 2, green) within their PPS or 5 cm (Distance 3, blue) or 15 cm (Distance 4, black) outside their PPS. (B) RTs to oddball stimuli as a function of sensory modality and distance at which stimuli was presented. Error bars indicate ±1 SEM.

modality: audio, visual, and audiovisual) × 4 (distance: 1–4) repeated-measures ANOVA on the average RTs to oddball presentations demonstrated a significant main effect of sensory modality, $F(2, 32) = 115.79$, $p < .001$, partial $\eta^2 = 0.879$, yet failed to revealed a difference across distances, $F(3, 48) = 0.815$, $p = .492$, or an interaction between these variables, $F(6, 96) = 0.257$, $p = .955$. As expected, on oddball trials, participants were faster to respond to audiovisual stimulus ($M = 297.68$ msec, $SEM = 11.18$ msec) than to either audio ($M = 338.22$ msec, $SEM = 12.15$ msec, $p = .017$, $d = 0.85$) or visual ($M = 405.63$ msec, $SEM = 11.65$ msec, $p < .001$, $d = 2.28$) stimulus, demonstrating a significant multisensory facilitation behavior. In addition to analyzing the raw RTs, these data were utilized to calculate absolute multisensory response enhancement (aMRE; e.g., Van der Stoep, Van der Stigchel, et al., 2016) according to Equation 1. This latter measure indicates whether the administration of multisensory stimuli veritably conveyed a behavioral benefit beyond the fact that a greater degree of sensory evidence was presented. Results revealed that, although a robust aMRE was present at all distances (all $ts > 4.53$, all $ps < .001$, all $ds > 1.09$, one-sample t test to zero), multisensory enhancement was not differently observed as a function of distance, $F(3, 48) = 0.352$, $p = .788$ (one-way repeated-measures ANOVA). Overall, thus, the behavioral data seemingly indicate that participants were attentive to the task at hand, and multisensory presentation was beneficial vis-à-vis its unisensory components irrespectively of distance.

$$aMRE = \min(RT_A, RT_V) - RT_{AV} \qquad (1)$$

Topography

Regarding topographical distributions at the sensor level, a 3 (sensory modalities) × 4 (distances) topographic ANOVA indicated several time periods in which there was a main effect of sensory modality: 54–74, 140–150, 166–178, and 192 msec poststimulus onset onwards. Importantly, this analysis did not reveal a dissimilarity in topography as a consequence of the distance at which the sensory stimuli were presented (all $ps > .105$), nor an interaction between these variables (all $ps > .135$). Given that the focus of interest here was in examining the impact of spatial location on the processing of stimuli in the different sensory modalities, topographic analyses were not pursued further.

Neural Strength

A 3 (sensory modalities) × 4 (distance) repeated-measures ANOVA on the GFP of the EEG signal demonstrated a significant main effect of distance between 344 and 361 msec poststimulus onset ($p < .01$ for at least 10 consecutive time points), a significant main effect of sensory modality 185–413 msec poststimulus onset ($p < .01$ for at least 10 consecutive time points), and a significant Distance × Sensory modality interaction between 323 and 371 msec poststimulus onset ($p < .01$ for at least 10 consecutive time points). To elucidate the origin of the significant interaction, we subsequently performed one-way repeated-measures ANOVAs for each sensory modality, independently and across distances. These ANOVAs did not demonstrate a significant difference across distances for either the audio or visual conditions (although this latter one showed a trend; see Figure 2)
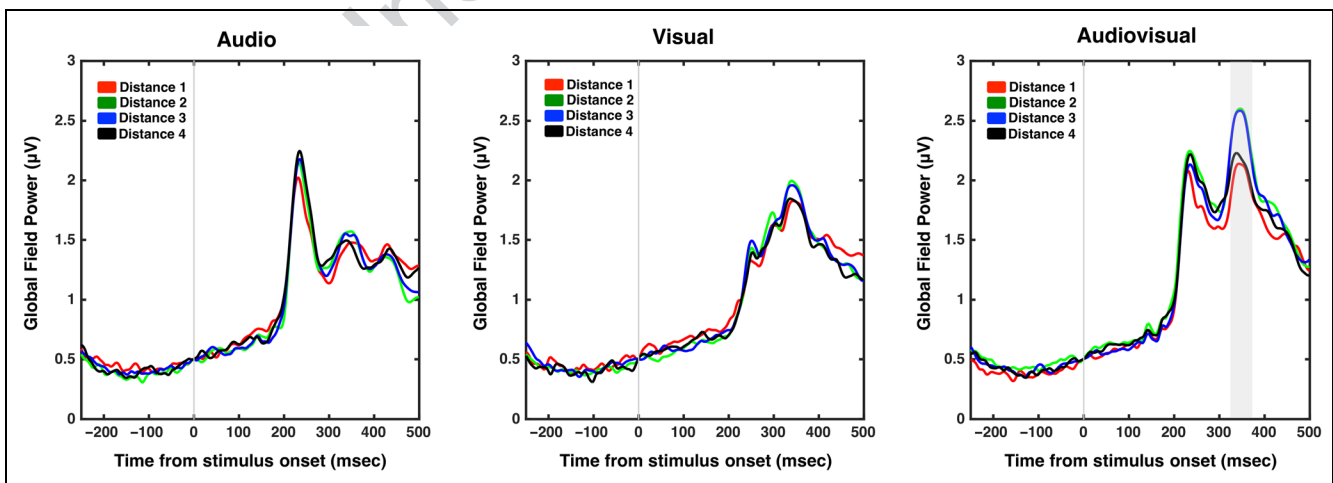

Figure 2. GFP as a function of sensory modality and distance. The presentation of auditory (leftmost), visual (center), and audiovisual (rightmost) stimuli all elicited reliable GFP changes from baseline (-250 to 0 msec on the x-axis). There was no significant modulation of GFP strength as a function of distance for the auditory or visual conditions, but in the audiovisual case GFP was significantly higher for distances near the boundary of PPS (Distances 2 and 3; green and blue, respectively) than for distances far from the boundary of PPS (Distances 1 and 4; red and black, respectively). The area highlighted in gray indicates the time points of significant difference ($p < .01$ for at least 10 consecutive time points; between 323 and 371 msec poststimulus onset).
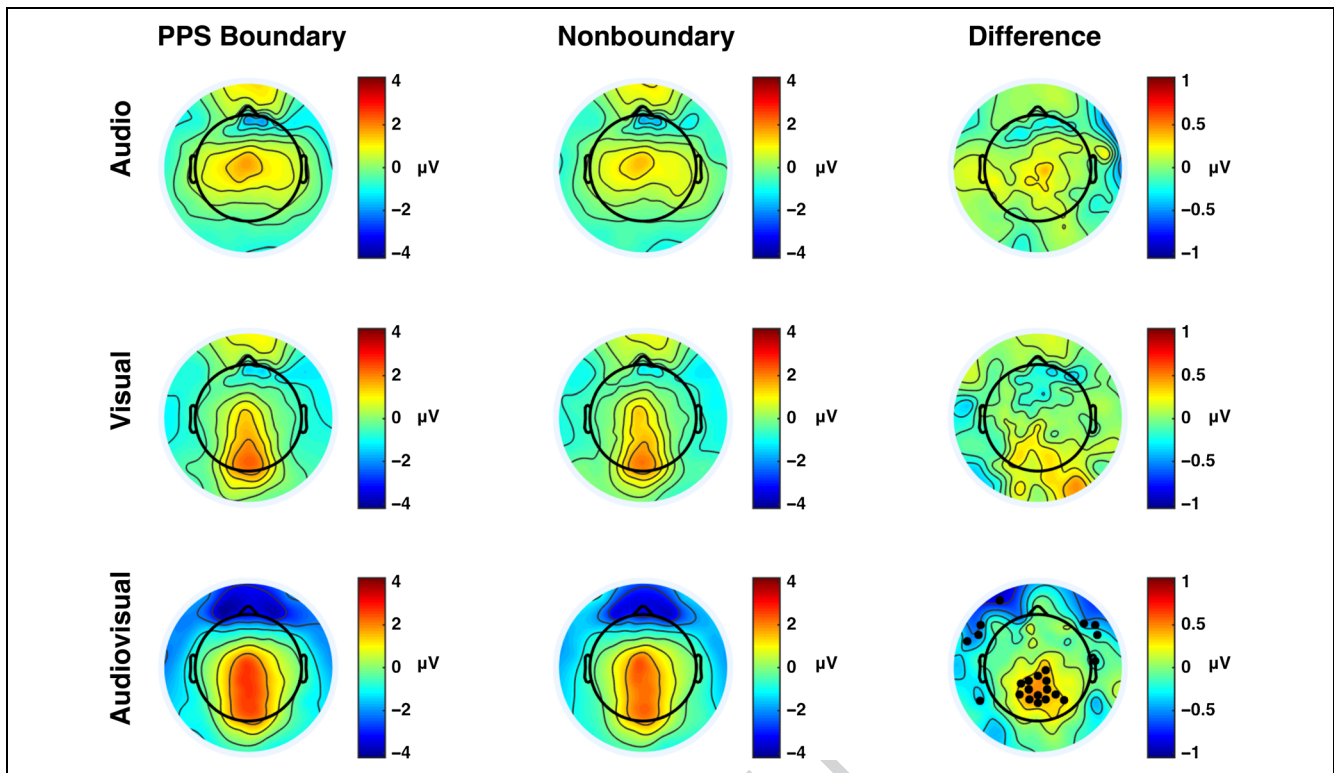
Figure 3. Topographic distributions. Topographic distributions of voltages during the GFP difference time period (323–371 msec) for audio (top row), visual (middle row), and audiovisual (bottom row) stimuli as a function of whether stimuli were presented near (leftmost column) or far (middle column) from the PPS boundary. The rightmost column shows the difference (PPS boundary − Nonboundary) between when stimuli were presented near versus far from the boundary of PPS. Highlighted electrodes in black (bottom right corner) are those that show a significant difference between conditions.

but did show a significant divergence in GFP in the multisensory condition within the interval between 321 and 372 msec poststimulus onset ($p < .01$ for at least 10 consecutive time points).

More specifically, as illustrated in Figure 2 (area highlighted in gray), during this interval, GFP was significantly higher in the multisensory condition for Distances 2 ($M = 2.45$ μV, $SEM = 0.22$ μV) and 3 ($M = 2.44$ μV, $SEM = 0.20$ μV), when compared with Distances 1 ($M = 2.02$ μV, $SEM = 0.20$ μV) and 4 ($M = 2.12$ μV, $SEM = 0.17$ μV; all significant ps $< .026$, all ds > 0.40). No difference was observed between the two distances close to the boundary of PPS (Distance 2 vs. Distance 3, $p = .99$) or between the two distances far from the boundary of PPS (Distance 1 vs. Distance 4, $p = 1.00$).

Given the clear difference in neural strength between stimuli presented near versus far from the PPS boundary, for subsequent steps we grouped data as a function of whether sensory stimuli had been presented at the boundary of PPS (Distances 2 and 3) or far from the boundary (Distances 1 and 4). We consider this approach appropriate given the need to enhance signal-to-noise ratios for ensuing analyses (i.e., source estimations, see below) and is analytically no different from collapsing across nonsignificant variables in analyses of variance—a very common approach. However, it must be emphasized that

this is a data-driven, as opposed to hypothesis-driven, approach to the analyses.

Averaging voltages across trials (i.e., calculating ERPs) during the time period of GFP significance (between 323 and 371 msec poststimulus onset) demonstrated once again no difference in either the audio (Figure 3, top row) or visual condition (Figure 3, middle row) but did show a significant difference in voltage for the multisensory condition (Figure 3, bottom row) as a function of distance. The electrodes that appeared to be driving this GFP difference ($p < .01$) had a central/posterior parietal distribution at the sensor level (see below for source localization of this dipole and the Appendix for time course of event potentials).

Neural Variability

In addition to revealing increase in neural strength (GFP) in response to multisensory stimuli when they are presented at the boundary of PPS (as opposed to far from the boundary), we wanted to delve further into the possible mechanistic basis of this difference. In this context, a reduction in neural firing variance (i.e., increase in reliability) is routinely present as firing rates increase (Churchland et al., 2006, 2010). Furthermore, specifically in the context of multisensory space coding, Ferri et al.

(2015) have recently demonstrated that the intertrial variance in the premotor cortex BOLD signal as measured by fMRI is strongly associated with interindividual difference in PPS size. Hence, in the current work, we analyzed the intertrial variance associated with presentation of audio, visual, or audiovisual stimulus either at the boundary of PPS or far from the PPS boundary in electrodes responsible for the GFP difference (see Methods for details and the Appendix for variance analysis on electrodes not demonstrating the GFP difference; Figures A2 and A3). As illustrated in Figure 4, the intertrial variance in EEG responses tended to increase quasimonotonically after stimulus onset. Interestingly, a 3 (sensory modalities) × 2 (PPS boundary vs. nonboundary) repeated-measures ANOVA demonstrated a significant main effect of distance between 352 and 401 msec poststimulus onset ($p < .01$ for at least 10 consecutive time points), with the variance being significantly reduced at the boundary of PPS. The analysis also revealed a significant main effect of sensory modality in the interval between 229 and 269 msec poststimulus onset and most importantly a significant Sensory Modality × Boundary/Nonboundary interaction between 234 and 301 msec poststimulus onset (all $ps < .01$ for at least 10 consecutive time points). Separate paired t tests, constrained within the period of significant interaction, but not averaged across time, revealed no significant difference (boundary vs. nonboundary) for the audio condition (all $ps > .012$) but did show a significant difference in the visual (between the time period 241 and 262 msec poststimulus onset; see Figure 4) and audiovisual (between 254 and 298 msec poststimulus onset; see Figure 4) conditions. Such a pattern of results suggests that the Sensory Modality × Distance interaction was driven initially by the visual condition and subsequently by the audiovisual condition. Furthermore, for both the visual and audiovisual conditions,

approximately 70 msec before the difference in GFP (for the multisensory condition), it appears that the variance in the EEG response was attenuated when stimuli were presented near the boundary of PPS. Within the multisensory condition, the gap between the end of the variance difference and the start of the GFP difference is of about 20 msec.

Source Estimation

Lastly, we performed source localization of the GFP difference exhibited in the multisensory condition (see above). The statistical contrast of inferred currents during AT presentation near versus far from PPS boundary during the sensor-level GFP difference identified two clusters of solution points as meeting our statistical criteria and thus likely to be accounting for the GFP difference. Both clusters indicated stronger current density values under conditions in which the multisensory stimuli were presented near the boundary of PPS (vs. far from the boundary). As illustrated in Figure 5A, a first cluster was identified in the right IPS (Talairach coordinates of peak, [35, −43, 49]), whereas the second was localized to the left insula ([−41, −13, 13]).

Furthermore, as depicted in Figure 5B (top row), the difference in activity to multisensory stimuli in the cluster localized to the IPS as a function of space (near PPS boundary subtracted from far from PPS boundary) during the time period of significant GFP difference (323–371 poststimulus onset) significantly correlated ($R = .56$, $p = .02$, Pearson correlation) on a subject-by-subject basis with the difference in variance observed approximately 70 msec beforehand (254–298 msec poststimulus onset) at the sensor level (averaged across sensors showing a significant voltage difference during the GFP difference time period). That is, the reduction in ERP variance
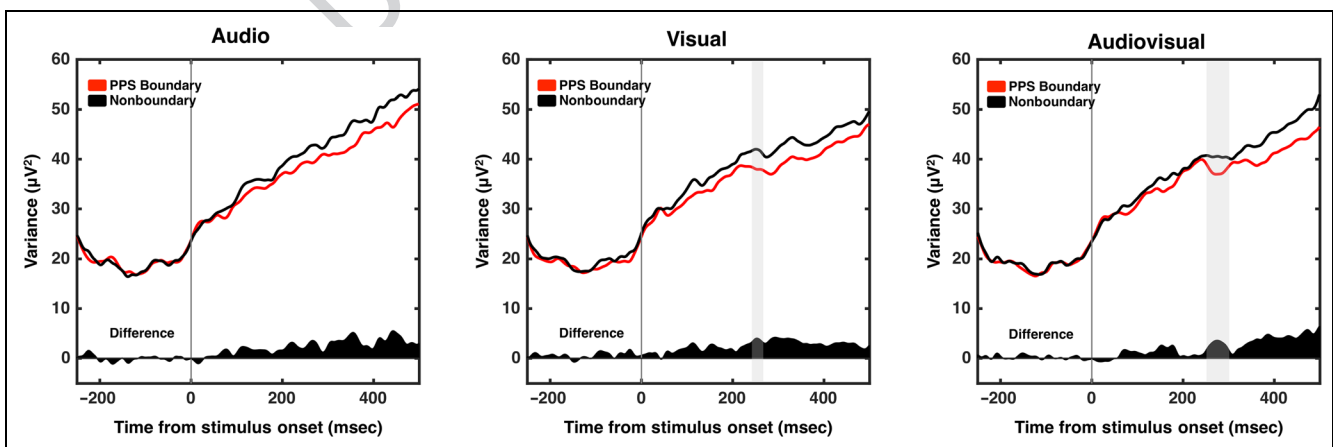

Figure 4. Variance of evoked responses. Variance of evoked responses as a function of sensory modality (audio leftmost, visual center, and audiovisual rightmost) and of whether stimuli were presented near (red) or far (black) from the PPS boundary. Results indicate a significant interaction between sensory modality and distance, which is driven by differences between distances in the visual (gray area in visual panel) and audiovisual (gray area in the audiovisual panel) conditions. The dark area plotted on the bottom of each panel is the difference between PPS boundary and nonboundary conditions.
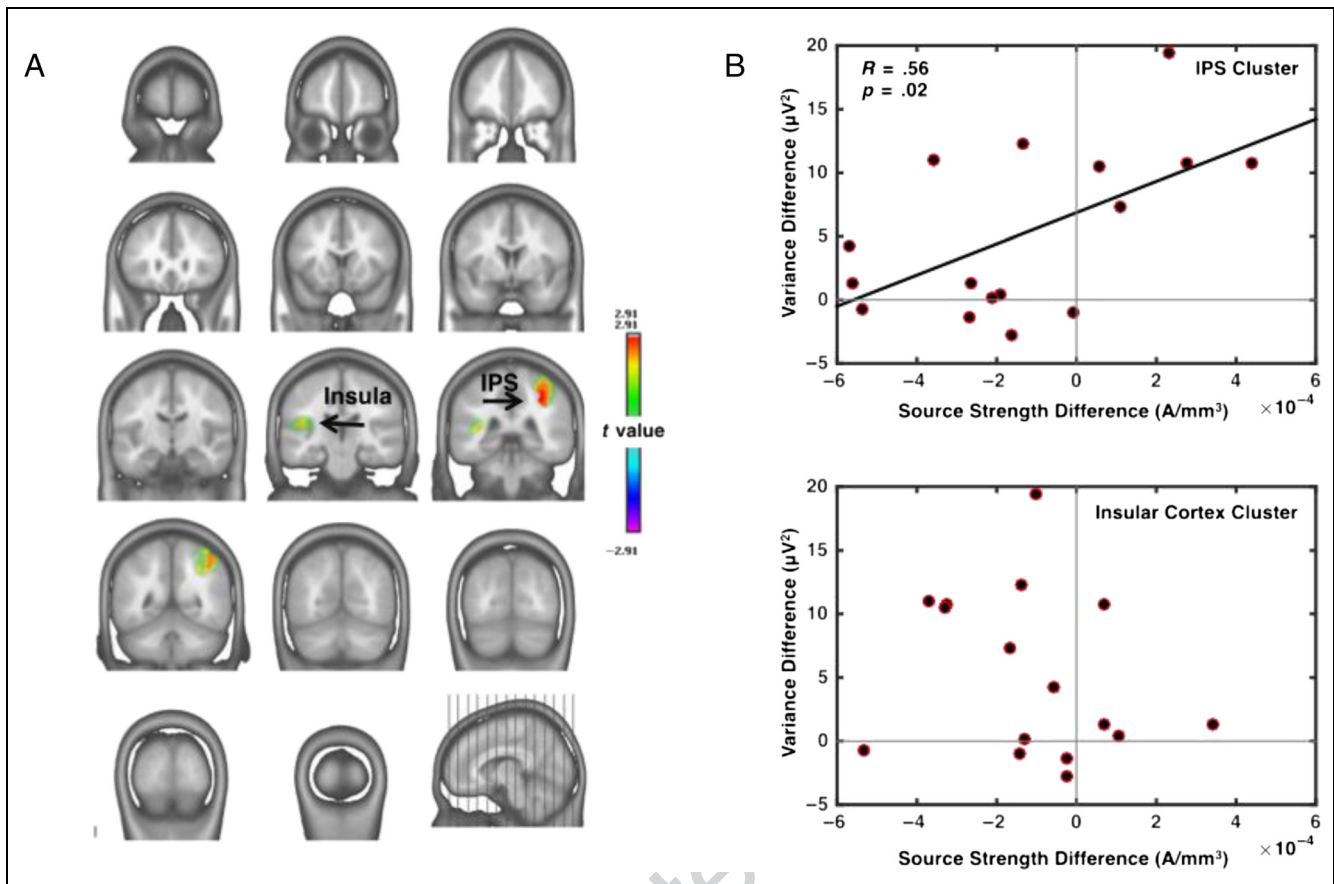
Figure 5. Source estimation of GFP difference and relation to sensor-level variance reduction. (A) The difference (far from minus near PPS boundary) in GFP values for multisensory stimuli as a function of whether they were presented near or far from the boundary of PPS was localized to the right IPS and the left insula. (B) The difference in current source density values (i.e., source strength difference − x-axis) for PPS boundary versus nonboundary conditions in the IPS (top) but not insula (bottom) was positively correlated with the reduction in variance of evoked responses to multisensory stimuli at the sensor level from (i.e., variance difference − y-axis).

seen under conditions in which multisensory stimuli were presented close to the boundary of PPS (vs. far from the boundary) is positively correlated with the increase in neural current inferred to be occurring in the IPS 70 msec later. These same correlations do not hold for the cluster localized to the insular cortex (bottom row; $R = -.44$, $p = .08$). Similarly, these correlations also do not hold for the reduction in variance seen during visual stimuli presentation (IPS cluster correlation: $R = -.17$, $p = .52$; insular cortex correlation: $R = -.20$, $p = .44$).

Brain–Behavior Relation

Although at a group level, distance did not appear to differentially impact multisensory oddball detection, the above-stated analysis (see Behavior section) was not performed as a function of distance to the PPS boundary (i.e., Distances 2 and 3 vs. Distances 1 and 4) but as a function of absolute distance (i.e., Distance 1 vs. Distance 2 vs. Distance 3 vs. Distance 4). Furthermore, even if at the group level there was no significant impact of distance— likely due to the very limited number of oddball

repetitions (20 repetitions per condition and distance spaced over the 2.5-hr duration of the experiment)—it is possible that neural responses may explain interindividual variance. Hence, RTs were compiled as a function of distance from PPS boundary, and aMRE was calculated. Furthermore, the impact of distance was evaluated by subtracting the aMRE at the PPS boundary from the aMRE far from the PPS boundary. The resulting value (in msec on the y axis in Figure 6) was correlated to the electrical current change inferred in IPS and insula as a function of PPS boundary–distance, as well as to the change in ERP variance at the electrodes driving the GFP difference (highlighted in Figure 3; black dots). Results were non-significant yet show a strong positive trend ($R = .45$, $p = .07$) relating inferred differential activity in IPS (near vs. far from PPS boundary) to differential aMRE (near vs. far from boundary). That is, seemingly the more the inferred neural activity in IPS was increased when stimuli were administered at the boundary of PPS (vs. far from it), the more did behavior benefit from placing audio-visual stimuli near the boundary of PPS. There was no relation between the reduction in sensor-level variance
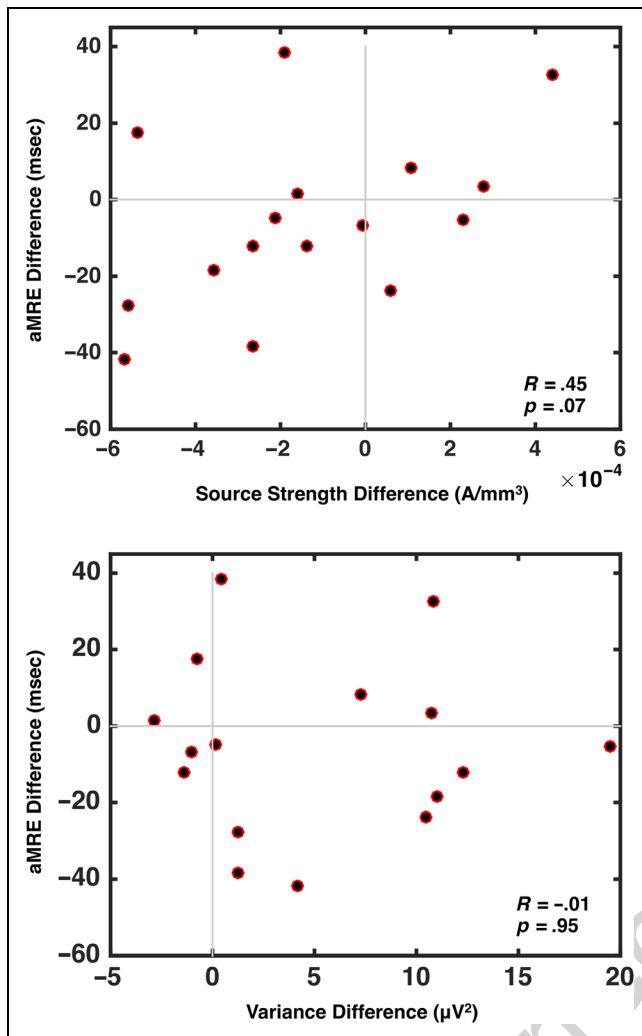
Figure 6. Brain–behavior correlation. Top: Correlation between (i) the difference in neural activity level to multisensory presentation in IPS as a function of the stimuli being close to or far from the boundary of PPS (far minus near subtraction; *x*-axis) and (ii) the difference in aMRE observed as a function of stimuli being presented near or far from the PPS boundary (far minus near subtraction; *y*-axis). The correlation was nonsignificant yet demonstrated a strong trend. Bottom: Similar to the top panel when indexing sensor-level variance as opposed to neural activity in IPS. Each dot represents a participant.

at the boundary of PPS and aMRE to stimuli presented at the mentioned distance ($R = -.01$, $p = .95$).

DISCUSSION

We recorded EEG data from participants observing audio, visual, and audiovisual stimuli presentations at different distances—both within and beyond their spatial reaching limit (a rough index of PPS; Patané et al., 2016, 2017; Bourgeois et al., 2014; Valdés-Conroy et al., 2014)—to characterize global changes in EEG power and variance associated with the presentation of unisensory auditory and visual, as well as multisensory audiovisual stimuli

within and beyond the PPS. The work was predicated on prior neuroimaging and neurophysiological studies focused on the neural instantiation of the PPS and employs high-density EEG in an effort to better understand the global network dynamics associated with the encoding of stimuli within, outside, and at the PPS boundary, when examined under both unisensory (visual alone, audio alone) and multisensory (combined audiovisual) conditions. In contrast to the vast majority of prior studies on PPS—employing either audiotactile or visuotactile pairings—and/or the reaching boundary—employing visual stimuli—here we use audiovisual stimuli. This permits us to question whether the PPS/reaching space demonstrates differential multisensory processing than the extrapersonal space above and beyond the association of the former space with the somatosensory system.

Overall, our results indicate that the global strength of neural response is accentuated when stimuli are presented at the boundary of PPS, as opposed to far from the boundary. This effect is surprising given prior work indicating enhanced multisensory processing within, as opposed to at the border of, the PPS (e.g., Serino et al., 2017; Spence, Pavani, & Driver, 2004; Spence, Pavani, Maravita, et al., 2004). This effect appears to be largest for multisensory (i.e., paired audiovisual) stimuli. The increase in neural strength occurred approximately 320 msec after stimulus onset, localized to centroparietal electrodes at the sensor level, and seemingly corresponds with neural generators in the (right) IPS and the (left) insular cortex at the source level. With regard to source localization, these results are in line with prior observations indicating the IPS (together with vPM) as the primary regions containing multisensory neurons with depth-restricted and bodily anchored receptive fields (e.g., Cléry, Guipponi, Wardak, & Ben Hamed, 2015; Brozzoli et al., 2012; Duhamel et al., 1998; see Grivaz et al., 2017, for a recent review and meta-analysis).

However, the reported effects are also strikingly different from the existing PPS literature. Namely, although much of the work has focused on visuotactile processes in the IPS (Schlack et al., 2005; Fogassi et al., 1996), there is also substantial evidence for audiovisual processes, the focus of the current study, taking place in this region (Werner & Noppeney, 2010; Saito et al., 2005; Calvert, 2001). Similarly, with regard to the insula, although it has only recently been directly associated with the encoding of PPS (Bernasconi et al., 2018), it is a known area of multisensory convergence (e.g., Rodgers, Benison, Klein, & Barth, 2008; audiovisual; Van der Wyk et al., 2010), and plays a pivotal role in bodily ownership (Salomon et al., 2016; Seth, 2013; Blanke, 2012), which in turn is arguably highly dependent on the representation of PPS (Noel, Blanke, & Serino, 2018; Noel, Cascio, Wallace, & Park, 2017; Salomon et al., 2017; Blanke, Slater, & Serino, 2015; Noel, Pfeiffer, et al., 2015). Thus, a question of

interest is: What is the role of audiovisual neurons and audiovisual distance-dependent representations in the PPS network? The findings appear to indicate that in contrast to audiotactile or visuotactile responses, which are largest near the body than far from the body, audiovisual processing is privileged near the boundary of PPS. In other words, although standard PPS experiments (e.g., Serino et al., 2015, 2017; Ferri et al., 2015) would predict differential processing between Distances 1 and 2 and between Distances 3 and 4, in the current setup we see differences between Distances 1 and 4 and between Distances 2 and 3, that is, near versus far from the PPS boundary. One possible interpretation of this pattern of results is that previous reports detailing enhanced multisensory processing in near space (vs. far space) during visuotactile/audiotactile stimulation are most likely driven by the fact that near conditions are more subject to the spatial principle of multisensory integration. Here, however, we see no evidence for enhanced audiovisual processing in near space (in fact, see Van der Stoep, Serino, et al., 2016; Van der Stoep, Van der Stigchel, et al., 2016; Van der Stoep et al., 2015, for evidence of enhanced audiovisual processing in the far space), and thus, it is unlikely that the PPS is a zone of privileged multisensory integration beyond the fact that stimuli presented in the PPS are presented near potential sites of somatosensory stimulation. Previous reports have demonstrated that audiotactile and visuotactile processing is facilitated in near space (e.g., Salomon et al., 2017; Noel, Grivaz, et al., 2015; Noel, Pfeiffer, et al., 2015), but this is likely to be a consequence of exteroceptive stimuli being placed within visuotactile/audiotactile receptive fields of PPS neurons when they are placed near the body. From this perspective, it makes a great deal of sense for visuotactile and audiotactile responses to be graded from the body outward—as these responses are anchored on the body (see Noel, Blanke, & Serino, 2018, for a similar argument). On the other hand, audiovisual responses are not anchored to the body, and thus, there is little reason for them to be enhanced near the body. However, there does appear to be a strong reason for differential audiovisual processing near (vs. far from) the PPS/reach boundary, as this represents the border of actionable space on audiovisual objects.

Interestingly, employing a visual-only task, Valdés-Conroy and colleagues (2014) report dorsal visual stream modulations in near space and ventral stream modulations in far space; that is, the encoding of visual features/objects is more sensitive in far space. Here we report an intermediate effect between classic audiotactile/visuotactile PPS effects—which are enhanced in the near space—and Valdés-Conroy et al.'s (2014) observation of more sensitive object-based visual processing in the far space (vs. location based in the near space). Thus, our findings indicating enhanced audiovisual processing at the PPS/reach boundary may suggest that the PPS/reach boundary not only differentiates between near and far space but also bridges between the ventral stream—primarily focused on the processing of exteroceptive objects—and the dorsal stream—primarily focused on spatial relations. In other words, the current results showing enhanced audiovisual processing at the PPS/reach boundary suggest a graded transition between the location where audiotactile and visuotactile pairings are enhanced (i.e., within the PPS), the location where audiovisual pairings are enhanced (i.e., at the boundary between the peripersonal and extrapersonal space/ reachable and nonreachable space), and finally, the location where vision is dominant (the extrapersonal space/nonreachable space). Importantly, here, as an approximation, we equate PPS with reaching space, but these spatial representations can be dissociated (see Cléry et al., 2015, for a discussion regarding similarities and distinctions between PPS and reaching space) and thus, in future work it will be important to determine whether the differential processing of certain sensory pairs is related to PPS, reaching space, or both.

From the temporal perspective, electrophysiology work indicates that feedforward visual projections reach IPS within approximately 100 msec of stimulus onset (Lamme & Roelfsema, 2000; Schmolesky et al., 1998; Felleman & Van Essen, 1991). Consistent with this timing, both Sambo and Foster (2009), who performed a visuotactile ERP study as a function of spatial disparity in depth (see also Bernasconi et al., 2018), and Valdés-Conroy et al. (2014), who performed a visual ERP study as a function of visual depth, report significant amplitude modulations in evoked responses within 100–200 msec of stimulus onset. In striking contrast, the present results show GFP differences that occur substantially later (i.e., between 320 and 370 msec) than would be predicted based on such feedforward projections. One possible explanation for these timing differences could lie in the sensory modalities stimulated: visuotactile versus audiovisual. Indeed, when contrasted with either the visual or tactile modality, auditory information reaches IPS fairly late within its hierarchy (Rauschecker & Tian, 2000; Romanski et al., 1999; Rauschecker, 1998; Hyvärinen, 1982; Divac, Lavail, Rakic, & Winston, 1977; Pandya & Kuypers, 1969). A second and nonmutually exclusive explanation is that the reported GFP difference is a result of a feedback process rather than a feedforward process. Regardless, the different latencies between prior visuotactile (Sambo & Foster, 2009) and audiotactile (Bernasconi et al., 2018) PPS studies and the current audiovisual study suggest that different processes are involved, detecting stimuli potentially touching the body in the former cases versus processing external stimuli as a function of the potential for interaction in the latter.

The argument that the observed effects are a function of feedback processes is further bolstered by the second major finding of the study—that the electrodes driving

the GFP differences also show a significant reduction in variability (electrodes that do not drive the GFP modulation as a function of proximity to PPS boundary do not show a similar reduction in variability; see Appendix). Remarkably, this increase in reliability precedes changes in neural strength (i.e., GFP and current strength) by 70 msec and is seen in both the multisensory and visual conditions, but not in the auditory condition. That is, reduction in variance near the PPS boundary at the sensor level is observed in sensory modalities "fast" to reach the IPS (i.e., vision), but not in those (i.e., audition) only reaching the IPS after extensive unisensory processing. Further support for the fact that the observed GFP difference is due to feedback comes in the form of the finding that the participants who demonstrated the greatest changes in ERP reliability at the sensor level as a function of whether stimuli were presented near or far from the boundary of PPS are the same participants that show the greatest increase in later neural strength at the source (i.e., brain) level. We interpret these results as putative evidence for a reentrant network effect and a demonstration that the enhanced encoding of audiovisual stimuli at the boundary of PPS is a dynamical network effect. This interpretation is also supported by the lack of distance-related topographical differences. Namely, in audiotactile or visuotactile PPS experiments, we should expect a change in topography as a function of observer–stimulus distance, as near objects/events should recruit PPS neurons, whereas far stimuli should not. Here, given the lack of topographical differences, it seems likely that stimuli at near and far distances (and near and far from PPS boundary) utilized the same network configuration (i.e., generators). The effect seen is solely in the domain of response strength, which our results suggest is due to a reduction in response variability at earlier time points.

The findings reported here are novel in that they suggest that, although audiotactile or visuotactile interactions may be privileged within the PPS—seemingly due to the fact that multisensory body-anchored receptive fields exist—audiovisual interactions seem to be advantaged at the boundary of PPS. Thus, the reported effect likely does not directly rely on the firing of multisensory neurons with depth-restricted receptive fields—rate code—but is more likely a result of changes in neural dynamics—a temporal code. That is, we conceive of the increased reliability in ERP as indicating that the precise timing of neural signals plays a fundamental role in conveying a differentiation between the space near versus far from the PPS boundary. Indeed, this work is strongly concordant with recent fMRI findings pinpointing the IPS as a major node in the integration of audiovisual information (Rohe & Noppeney, 2015), in particular due to its role in modulating the reliability attributed to each of the sensory modalities in the neural instantiation of a Bayesian inference process (Rohe & Noppeney, 2016).

Lastly, it is interesting to contrast our findings with the recent demonstration that intertrial variability of the hemodynamic response function (i.e., BOLD) in vPM is associated with the interindividual variability in PPS size (Serino, 2016; Ferri et al., 2015). That is, although here we demonstrate reduced variability in ERPs at centroparietal electrodes as a factor encoding for the boundary of PPS, Ferri et al. (2015) show that an increase in neural variability in the vPM cortex predicts larger PPS representations. As Ferri et al. (2015) discuss, neural variability has routinely been associated with plastic and dynamic processes (Mandelblat-Cerf et al., 2009; Faisal et al., 2008; Rokni et al., 2007), and they argue that having a large dynamic range in variance is likely adaptive in allowing for a flexible remapping of PPS representation. In contrast, we show a reduction of variability selectively at the boundary of PPS and over centroparietal electrodes. We propose that the enhancement in neural reliability in these sensors may also be adaptive, as although variability in vPM may allow for flexibility in the overall size in PPS (Ferri et al., 2015) the greater neural reliability seen in centroparietal electrodes may assure the stable and sensitive processing of stimuli located around the boundary of PPS, that is, a portion of space particularly relevant for behavior (Graziano & Cooke, 2006). The contrasting effects on variance seen between vPM (i.e., Ferri et al., 2015) and centroparietal electrodes (i.e., here) may also be related to the more prominent functional roles of these nodes: Whereas vPM is likely to be more closely associated with encoding the motor aspects of the PPS (Avenanti, Annela, & Serino, 2012), the parietal cortex is more closely associated with encoding the sensory and perceptual features of PPS (Serino, Canzoneri, & Avenanti, 2011), in particular when an audiovisual, as opposed to visuotactile or audiotactile pairing, is utilized. Consequently, it may be of strong adaptive value to build stable and faithful perceptual representations of the objects and events that are at one's PPS boundary (demonstrated here), whereas it may be of strong adaptive value to more flexibly specify the motoric representation and response to these stimuli once they are within the PPS (as in Ferri et al., 2015).

In conclusion, we demonstrate that multisensory stimuli presented close to the boundary of PPS are associated with enhanced neural response strength in parietal electrodes that source localize to IPS and insula. Furthermore, results suggest that the increased strength of neural response is likely a result of recurrent network activity with strong feedback contributions, as the effect is seen relatively late and is preceded by an increase in ERP reliability. These results also raise a number of novel questions. For instance, the lack of a topographical effect as a function of distance suggests that audiovisual processing occurs within the same network regardless of distance (at least within the range of distances tested here). This apparent lack of recruitment of the "traditional" PPS network within the current study may also explain why

we observed no difference in behavioral performance as a function of distance. Thus, it remains an open question as to whether, and if so how and when, do the neuronal populations indexed here via an audiovisual task interact with the standard frontoparietal PPS network composed of visuotactile and audiotactile neurons. A limitation of the current study is that PPS was not measured via standard multisensory interaction tasks (see Serino et al., 2017; Spence, Pavani, & Driver, 2004; Spence, Pavani, Maravita, et al., 2004) but simply assumed to be approximately the size of participants' reach (see Patané et al., 2016, 2017; Bourgeois et al., 2014; Valdés-Conroy et al., 2014). In turn, it is possible that the distances indexed were either all too large or too small to include peripersonal and extrapersonal space. To better understand the interplay between the results uncovered here and PPS representation (i.e., whether the findings here apply to reach boundary and/or PPS boundary), in the future it will be interesting to examine within subjects the neural correlates of audiotactile, visuotactile, and audiovisual stimulus presentations as a function of distance. Scaffolded on the current findings, such a project would be hypothesis-driven (vs. largely data-driven here) and would be predicated on the expectation of distinct neural correlates for audiotactile and visuotactile stimuli presented within versus beyond the PPS (but not for audiovisual pairings) and distinct neural correlates for audiovisual (but not audiotactile or visuotactile) presentations near versus far from the PPS boundary. Similarly, given that alterations in neural responses as a function of distance are observed within the initial 100–200 msec for visuotactile pairings (Sambo & Foster, 2009), at approximately 200 msec for audiotactile pairings (Bernasconi et al., 2018), and at approximately 300 msec for audiovisual pairings, it would be interesting to examine if and how are these different multisensory distance-dependent effects related to one another.

Overall, our results emphasize the importance that 3-D space may have in multisensory processing above and beyond the delineation of the space near the body. Namely, the increase firing resulting from the recruitment of PPS neurons when stimuli are close to the body may not only directly affect visuotactile and audiotactile processing via the rate code but also indirectly alter the encoding of other multisensory pairings (i.e., audiovisual) via changes in temporal coding and neural dynamics.

APPENDIX

The main text details that between 323 and 371 msec poststimulus onset there is a significant distance by sensory modality interaction in GFP (Figure 2). Given post hoc tests demonstrating a clustering of distances near the PPS boundary versus those far from the PPS boundary, Conditions 1 and 4 are collapsed, as are Conditions 2 and 3. The ERP to multisensory stimulation during the significant GFP difference is then contrasted between near and far from PPS boundary distances. This analysis indicates that electrodes with a central/posterior parietal distribution drive the GFP difference. For completeness, here we extend this analysis to all time periods and illustrate ERPs at classically considered auditory (Figure A1, top row) and visual electrodes (Figure A1, middle row), as well as at an electrode showing the mentioned GFP difference (Figure A1, bottom row; Luck, 2014). For each electrode, we perform a time-resolved 4 (distances) × 3 (sensory modality; audio, visual, audiovisual) repeated-measures ANOVA. Regarding the auditory electrode (Figure A1, top, inset), results demonstrate a main effect of sensory modality between 201 and 271 msec poststimulus onset ($p < .01$), as well as between 340 and 454 msec poststimulus onset ($p < .01$). There was no main effect of distance nor an interaction between distance and modality of sensory stimulation. The visual electrode (Figure A1, middle, inset) showed a main effect of distance between 269 and 300 msec poststimulus onset ($p < .01$) and a main effect of sensory modality between 208 and 264 msec ($p < .01$), as well as between 318 and 471 msec poststimulus onset ($p < .01$). There was no interaction between distance and sensory modality at this electrode. Lastly, the centroparietal electrode (Figure A1, bottom, inset) demonstrated no main effect of distance but did show a main effect of sensory modality between 198–265, 277–362, and 404–474 msec poststimulus onset ($p < .01$). As expected given that this electrode was identified to be one of those driving the GFP effect reported in the main text, this electrode exhibited a sensory modality by distance interaction between 98–124 and 313–381 msec poststimulus onset ($p < .01$). Taken together, these results concord with the GFP analysis, each electrode showing primarily responses to their appropriate sensory modality, and with solely the centroparietal electrode—and not electrodes thought to reflect early sensory areas activity—demonstrating a sensory modality by distance interaction: a PPS effect. Of note, as it is evidenced in Figure A1 and the diverse response patterns across electrodes, this analysis is heavily reliant on the particular electrodes analyzed (and montage referencing). Thus, we draw stronger conclusions about the differential evoked responses as a consequence of modality of sensory stimulation and distance from the GFP analysis in the main text and this ERP analysis is corroborative.

The main text states that there is a reduction in the variance of evoked responses when visual (between the time period 241 and 262 msec poststimulus onset; see Figure 4) or audiovisual (between 254 and 298 msec poststimulus onset; Figure 4) stimuli are presented near the PPS boundary. Furthermore, the degree to which variance is reduced (at the level of electrodes) in the audiovisual case covaries with the estimated current difference localized to IPS between presentation near and far from

the PPS boundary (Figure 5). However, to further support the putative relation between the reduction of intertrial variance in centroparietal electrodes and current differences at the source level, we must broaden the scope to examine intertrial variance at all electrodes. To do so, as in the main text, we performed a 3 (sensory modalities) × 2 (PPS boundary vs. nonboundary) repeated-measures ANOVA on intertrial variance of all electrodes not driving the GFP difference between boundary and nonboundary (ERP analysis in Figure 3). At difference from the electrodes driving the GFP difference, this analysis showed no main effect of distance or modality of sensory stimulation nor an interaction between these variables (Figure A2). To ratify this finding,

we performed a repeated-measure ANOVA contrasting the difference time courses (boundary vs. nonboundary) for electrodes driving the GFP difference versus not, as a function of sensory modality (i.e., 3 [audio, visual, audiovisual] × 2 [GFP electrodes vs. non-GFP electrodes]). This analysis revealed no main effect of electrode type (GFP vs. non-GFP electrode) nor a main effect of sensory modality. However, there was a significant interaction between these variables between 264 and 288 msec post-stimulus onset. This interaction was driven by larger boundary versus nonboundary variance difference in the GFP than non-GFP electrodes in the visual and audiovisual modalities ($p < .01$), but not in the auditory sense (Figure A3).
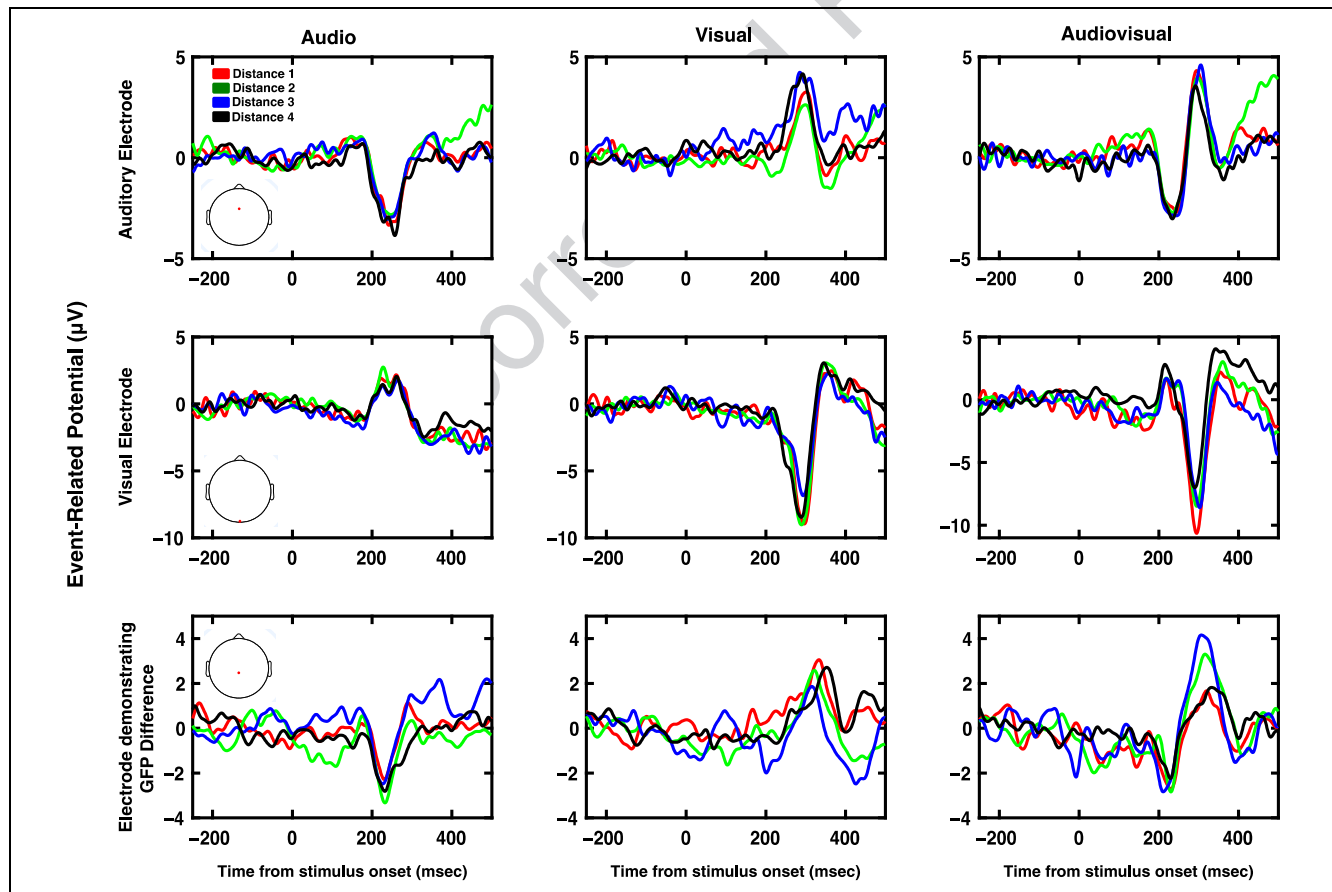

Figure A1. ERPs to auditory, visual, and audiovisual stimuli. Top: Auditory (leftmost column), visual (middle column), and audiovisual (rightmost column) ERPs as a function of distance (Distance 1 = red; Distance 2 = green; Distance 3 = blue; Distance 4 = black) at a frontocentral electrode (red dot in inset). Zero on *x*-axis denotes the time of stimulus onset. Middle: Follows conventions as for top panel, but ERPs are illustrated at an occipital electrode. Bottom: Follows conventions as for top/middle panels, but ERPs are illustrated at a centroparietal electrode driving the GFP difference (Figure 2). As for the GFP analysis, evoked potentials for Distances 2 and 3 show greater amplitude than those at Distances 1 and 4.
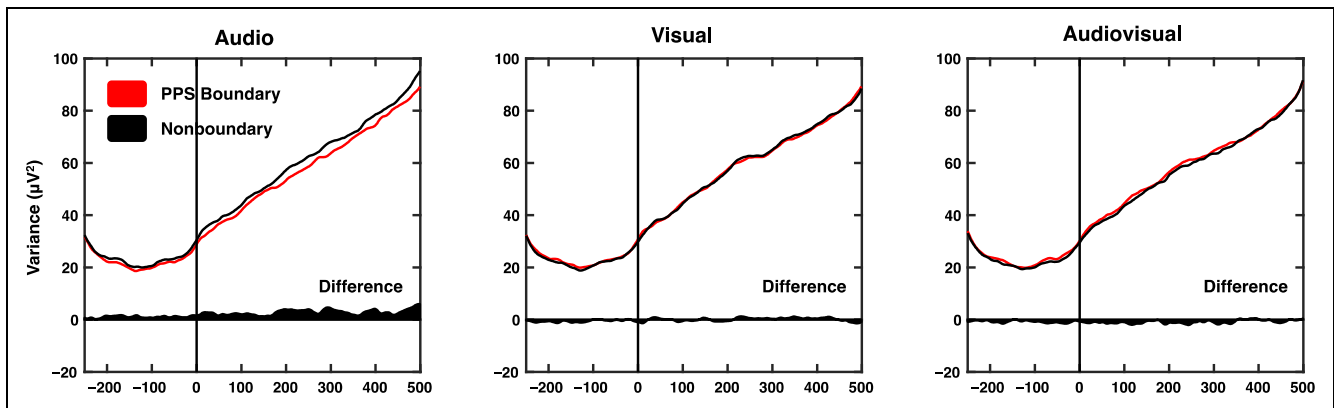
Figure A2. Variance of evoked responses at electrodes not driving GFP modulation as a function of distance to PPS boundary. Variance of evoked responses as a function of sensory modality (audio leftmost, visual center, and audiovisual rightmost) and of whether stimuli were presented near (red) or far (black) from the PPS boundary. Dark area plotted on the bottom of each panel is the difference between PPS boundary and nonboundary conditions.
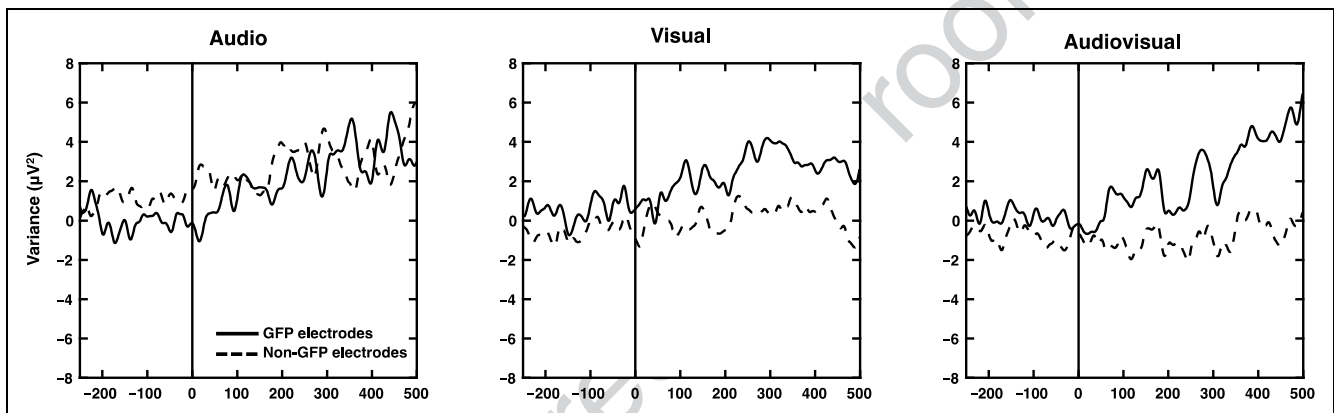

Figure A3. Contrast of the difference in ERP variance as a function of sensory modality and electrodes. Variance of evoked potentials to auditory (leftmost), visual (middle), and audiovisual (right) stimulation in centroparietal electrodes driving the GFP modulation as a function of distance to PPS boundary (solid black line; see Figure 3 for electrode location) and in electrodes not driving the mentioned GFP modulation (dashed black line).

UNCITED REFERENCES

Gonzalez Andino, 2009
Koenig & Melie-Garcia, 2010

Acknowledgments

REFERENCES

Avenanti, A., Annela, L., & Serino, A. (2012). Suppression of premotor cortex disrupts motor coding of peripersonal space. *Neuroimage*, *63*, 281–288.

Bernasconi, F., Noel, J. P., Park, H. D., Seeck, M., Spinelli, L., Blanke, O., et al. (2018). Evidence for a multisensory peripersonal space in humans: An intracranial EEG study. *Cerebral Cortex*.

Berti, A., & Frassinetti, F. (2000). When far becomes near: Re-mapping of space by tool-use. *Journal of Cognitive Neuroscience*, *12*, 415–420.

Blanke, O. (2012). Multisensory brain mechanisms of bodily self-consciousness. *Nature Reviews Neuroscience*, *13*, 556–571.

Blanke, O., Slater, M., & Serino, A. (2015). Behavioral, neural, and computational principles of bodily self-consciousness. *Neuron*, *88*, 145–166.

Bourgeois, J., Farne, A., & Coello, Y. (2014). Costs and benefits of tool-use on the perception of reachable space. *Acta Psychologica (Amsterdam)*, *148*, 91–95.

Bremmer, F., Schlack, A., Shah, N. J., Zafiris, O., Kubischik, M., Hoffmann, K., et al. (2001). Polymodal motion processing in posterior parietal and premotor cortex: A human fMRI study strongly implies equivalencies between humans and monkeys. *Neuron*, *29*, 287–296.

Brozzoli, C., Gentile, G., & Ehrsson, H. H. (2012). That's near my hand! Parietal and premotor coding of hand-centered space contributes to localization and self-attribution of the hand. *Journal of Neuroscience*, *32*, 14573–14582.

Brozzoli, C., Gentile, G., Petkova, V. I., & Ehrsson, H. H. (2011). fMRI adaptation reveals a cortical mechanism for the coding of space near the hand. *Journal of Neuroscience*, *31*, 9023–9031.

Calvert, G. A. (2001). Cross modal processing in the human brain: Insights from functional neuroimaging studies. *Cerebral Cortex*, *11*, 1110–1123.

Cappe, C., Thut, G., Romei, V., & Murray, M. M. (2010). Auditory-visual multisensory interactions in humans: Timing, topography, directionality, and sources. *Journal of Neuroscience*, *30*, 12572–12580.

Churchland, M. M., Yu, B. M., Cunningham, J. P., Sugrue, L. P., Cohen, M. R., Corrado, G. S., et al. (2010). Stimulus onset quenches neural variability: A widespread cortical phenomenon. *Nature Neuroscience*, *13*, 369–378.

Churchland, M. M., Yu, B. M., Ryu, S. I., Santhanam, G., & Shenoy, K. V. (2006). Neural variability in premotor cortex provides a signature of motor preparation. *Journal of Neuroscience*, *26*, 3697–3712.

Cléry, J., Guipponi, O., Wardak, C., & Ben Hamed, S. (2015). Neuronal bases of peripersonal and extrapersonal spaces, their plasticity and their dynamics: Knowns and unknowns. *Neuropsychologia*, *70*, 313–326.

Corveleyn, X., Lopez-Moliner, J., & Coello, Y. (2015). Temporal and spatial constraints of action effect on sensory binding. *Experimental Brain Research*, *233*, 3379–3392.

de Haan, A. M., Smit, M., van der Stigchel, S., & Dijkerman, H. C. (2016). Approaching threat modulates visuotactile interactions in peripersonal space. *Experimental Brain Research*, *234*, 1875–1884.

De Lucia, M., Clarke, S., & Murray, M. M. (2010). A temporal hierarchy for conspecific vocalization discrimination in humans. *Journal of Neuroscience*, *30*, 11210–11221.

de Vignemont, F., & Iannetti, G. D. (2015). How many peripersonal spaces? *Neuropsychologia*, *70*, 327–334.

di Pellegrino, G., Làdavas, E., & Farnè, A. (1997). Seeing where your hands are. *Nature*, *388*, 730.

Divac, I., Lavail, J. H., Rakic, P., & Winston, K. R. (1977). Heterogeneous afferents to the inferior parietal lobule of the rhesus monkey revealed by the retrograde transport method. *Brain Research*, *123*, 197–207.

Duhamel, J. R., Bremmer, F., Ben Hamed, S., & Graf, W. (1997). Spatial invariance of visual receptive fields in parietal cortex neurons. *Nature*, *389*, 845–848.

Faisal, A. A., Selen, L. P., & Wolpert, D. M. (2008). Noise in the nervous system. *Nature Reviews Neuroscience*, *9*, 292–303.

Farnè, A., & Ladavas, E. (2000). Dynamic size-change of hand peripersonal space following tool use. *NeuroReport*, *11*, 1645–1649.

Farnè, A., & Làdavas, E. (2002). Auditory peripersonal space in humans. *Journal of Cognitive Neuroscience*, *14*, 1030–1043.

Farnè, A., Pavani, F., Meneghello, F., & Ladavas, E. (2000). Left tactile extinction following visual stimulation of a rubber hand. *Brain*, *123*, 2350–2360.

Felleman, D. J., & Van Essen, D. C. (1991). Distributed hierarchical processing in the primate cerebral cortex. *Cerebral Cortex*, *1*, 1–47.

Ferri, F., Huang, Z., Perrucci, M. G., Ferretti, F., Romani, G. L., & Northoff, G. (2015). Intertrial variability in the premotor cortex accounts for individual differences in peripersonal space. *Journal of Neuroscience*, *35*, 16328–16339.

Fogassi, L., Gallese, V., Fadiga, L., Luppino, G., Matelli, M., & Rizzolatti, G. (1996). Coding of peripersonal space in inferior premotor cortex (area F4). *Journal of Neurophysiology*, *76*, 141–157.

Foxe, J. J., Morocz, I. A., Murray, M. M., Higgins, B. A., Javitt, D. C., & Schroeder, C. E. (2000). Multisensory auditory-somatosensory interactions in early cortical processing revealed by high-density electrical mapping. *Cognitive Brain Research*, *10*, 77–83.

Fryar, C. D., Gu, Q., Ogden, C. L., & Flegal, K. M. (2016). Anthropometric reference data for children and adults: United States, 2011–2014. *Vital and Health Statistics*, *3*, 1–46.

Galli, G., Noel, J. P., Canzoneri, E., Blanke, O., & Serino, A. (2015). The wheelchair as a full-body tool extending the peripersonal space. *Frontiers in Psychology*, *6*, 639.

Gentile, G., Petkova, V. I., & Ehrsson, H. H. (2011). Integration of visual and tactile signals from the hand in the human brain: An fMRI study. *Journal of Neurophysiology*, *105*, 910–922.

Ghazanfar, A. A., & Schroeder, C. E. (2006). Is neocortex essentially multisensory? *Trends in Cognitive Sciences*, *10*, 278–285.

Gonzalez Andino, S. L. (2009). Methods for determining frequency- and region-dependent relationships between estimated LFPs and BOLD responses in humans. *Journal of Neurophysiology*, *101*, 491–502.

Gonzalez Andino, S. L., Murray, M. M., Foxe, J. J., & de Peralta Menendez, R. G. (2005). How single-trial electrical neuroimaging contributes to multisensory research. *Experimental Brain Research*, *166*, 298–304.

Gordon, C. C., Churchill, T., Clauser, C. E., Bradtmiller, B., McConville, J. T., Tebbetts, I., et al. (1989). *Anthropometric survey of US Army personnel: Summary statistics, interim report for 1988*. Yellow Springs, OH: Anthropology Research Project.

Grave de Peralta Menendez, R., Gonzalez Andino, S., Lantz, G., Michel, C. M., & Landis, T. (2001). Noninvasive localization of electromagnetic epileptic activity. I. Method descriptions and simulations. *Brain Topography*, *14*, 131–137.

Grave de Peralta Menendez, R., Murray, M. M., Michel, C. M., Martuzzi, R., & Gonzalez Andino, S. L. (2004). Electrical neuroimaging based on biophysical constraints. *Neuroimage*, *21*, 527–539.

Graziano, M. S., & Cooke, D. F. (2006). Parieto-frontal interactions, personal space, and defensive behavior. *Neuropsychologia*, *44*, 2621–2635.

Graziano, M. S., Hu, X. T., & Gross, C. G. (1997). Coding the locations of objects in the dark. *Science*, *277*, 239–241.

Graziano, M. S., Reiss, L. A., & Gross, C. G. (1999). A neuronal representation of the location of nearby sounds. *Nature*, *397*, 428–430.

Hyvärinen, J. (1982). *The parietal cortex of monkey and man*. Berlin: Springer-Verlag.

Kandula, M., van der Stoep, N., Hofman, D., & Dijkerman, H. C. (2017). On the contribution of overt tactile expectations to visuotactile interactions within the peripersonal space. *Experimental Brain Research*, *235*, 2511–2522.

Knebel, J. F., & Murray, M. M. (2012). Towards a resolution of conflicting models of illusory contour processing in humans. *Neuroimage*, *59*, 2808–2817.

Knill, D. C., & Pouget, A. (2004). The Bayesian brain: The role of uncertainty in neural coding and computation. *Trends in Neurosciences*, *27*, 712–719.

Koenig, T., & Melie-Garcia, L. (2010). A method to determine the presence of averaged event-related fields using randomization tests. *Brain Topography*, *23*, 233–242.

Làdavas, E. (2002). Functional and dynamic properties of visual peripersonal space. *Trends in Cognitive Sciences*, *6*, 17–22.

Làdavas, E., di Pellegrino, G., Farnè, A., & Zeloni, G. (1998). Neuropsychological evidence of an integrated visuotactile representation of peripersonal space in humans. *Journal of Cognitive Neuroscience*, *10*, 581–589.

Lamme, V. A., & Roelfsema, P. R. (2000). The distinct modes of vision offered by feedforward and recurrent processing. *Trends in Neurosciences*, *23*, 571–579.

Lehmann, D. (1987). Principles of spatial analysis. In A. S. Gevins & A. Remond (Eds.), *Handbook of electroencephalography and clinical neurophysiology: Methods of analysis of brain electrical and magnetic signals* (Vol. 1, pp. 309–354). Amsterdam: Elsevier.

Lehmann, D., & Skrandies, W. (1980). Reference-free identification of components of checkerboard evoked multichannel potential fields. *Electroencephalography and Clinical Neurophysiology*, 48, 609–621.

Leys, C., Ley, C., Klein, O., Bernard, P., & Licata, L. (2013). Detecting outliers: Do not use standard deviation around the mean, use absolute deviation around the median. *Journal of Experimental Social Psychology*, 49, 764e6.

Luck, S. J. (2014). *An introduction to the event-related potential technique*. Cambridge, MA: MIT Press.

Macaluso, E., & Maravita, A. (2010). The representation of space near the body through touch and vision. *Neuropsychologia*, 48, 782–795.

Makin, T. R., Holmes, N. P., & Zohary, E. (2007). Is that near my hand? Multisensory representation of peripersonal space in human intraparietal sulcus. *Journal of Neuroscience*, 27, 731–740.

Mandelblat-Cerf, Y., Paz, R., & Vaadia, E. (2009). Trial-to-trial variability of single cells in motor cortices is dynamically modified during visuomotor adaptation. *Journal of Neuroscience*, 29, 15053–15062.

Maravita, A., Spence, C., & Driver, J. (2003). Multisensory integration and the body schema: Close to hand and within reach. *Current Biology*, 13, R531–R539.

Martuzzi, R., Murray, M. M., Meuli, R. A., Thiran, J.-P., Maeder, P. P., Michel, C. M., et al. (2009). Methods for determining frequency- and region-dependent relationships between estimated LFPs and BOLD responses in humans. *Journal of Neurophysiology*, 101, 491–502.

Meredith, M. A., & Stein, B. E. (1996). Spatial determinants of multisensory integration in cat superior colliculus neurons. *Journal of Neurophysiology*, 75, 1843–1857.

Michel, C. M., Murray, M. M., Lantz, G., Gonzalez, S., Spinelli, L., & Grave de Peralta, R. (2004). EEG source imaging. *Clinical Neurophysiology*, 115, 2195–2222.

Milne, E. (2011). Increased intra-participant variability in children with autistic spectrum disorders: Evidence from single-trial analysis of evoked EEG. *Frontiers in Psychology*, 2, 51.

Molholm, S., Ritter, W., Murray, M. M., Javitt, D. C., Schroeder, C. E., & Foxe, J. J. (2002). Multisensory auditory-visual interactions during early sensory processing in humans: A high-density electrical mapping study. *Brain Research, Cognitive Brain Research*, 14, 115–128.

Murray, M. M., Brunet, D., & Michel, C. M. (2008). Topographic ERP analyses: A step-by-step tutorial review. *Brain Topography*, 20, 249–264.

Murray, M. M., & Wallace, M. T. (2012). *The neural bases of multisensory processes*. Boca Raton, FL: CRC Press.

Noel, J. P., Blanke, O., Magosso, E., & Serino, A. (2018). Neural adaptation accounts for the dynamic resizing or peripersonal space: Evidence from a psychophysical-computational approach. *Journal of Neurophysiology*, 119, 2307–2333.

Noel, J. P., Blanke, O., & Serino, A. (2018). From multisensory integration in peripersonal space to bodily self-consciousness: From statistical regularities to statistical inference. *Annals of the New York Academy of Science*. doi:10.1111/nyas.13867.

Noel, J. P., Cascio, C., Wallace, M., & Park, S. (2017). The spatial self in schizophrenia and autism spectrum disorder. *Schizophrenia Research*, 179, 8–12.

Noel, J. P., Grivaz, P., Marmaroli, P., Lissek, H., Blanke, O., & Serino, A. (2015). Full body action remapping of peripersonal space: The case of walking. *Neuropsychologia*, 70, 375–384.

Noel, J. P., Lukowska, M., Wallace, M. T., & Serino, A. (2016). Multisensory simultaneity judgment and proximity to the body. *Journal of Vision*, 16, 21.

Noel, J. P., Modi, K., Wallace, M., & Van der Stoep, N. (2018). Audiovisual integration in depth: Multisensory binding and gain as a function of distance. *Experimental Brain Research*, 236, 1939–1951.

Noel, J. P., Park, H. D., Pasqualini, I., Lissek, H., Wallace, M., Blanke, O., et al. (2018). Audio–visual sensory deprivation degrades visuotactile peripersonal space. *Consciousness and Cognition*, 61, 61–75.

Noel, J. P., Pfeiffer, C., Blanke, O., & Serino, A. (2015). Full body peripersonal space as the space of the bodily self. *Cognition*, 144, 49–57.

Noel, J. P., Simon, D., Thelen, A., Maier, A., Blake, R., & Wallace, M. (2018). Probing electrophysiological indices of perceptual awareness across unisensory and multisensory modalities. *Journal of Cognitive Neuroscience*, 30, 814–828.

Occelli, V., Spence, C., & Zampini, M. (2011). Audiotactile interactions in front and rear space. *Neuroscience and Biobehavioral Reviews*, 35, 589–598.

Pandya, D. N., & Kuypers, H. G. (1969). Cortico-cortical connections in the rhesus monkey. *Brain Research*, 13, 13–36.

Patané, I., Farnè, A., & Frassinetti, F. (2017). Cooperative tool-use reveals peripersonal and interpersonal spaces are dissociable. *Cognition*, 166, 13–22.

Patané, I., Iachini, T., Farnè, A., & Frassinetti, F. (2016). Disentangling action from social space: Tool-use differently shapes the space around us. *PLoS ONE*, 11, e0154247.

Pavani, F., & Castiello, U. (2004). Binding personal and extrapersonal space through body shadows. *Nature Neuroscience*, 7, 14–16.

Pfeiffer, C., Noel, J. P., Serino, A., & Blanke, O. (2018). Vestibular modulation of peripersonal space boundaries. *European Journal of Neuroscience*, 47, 800–811.

Rauschecker, J. P. (1998). Cortical processing of complex sounds. *Current Opinion in Neurobiology*, 8, 516–521.

Rauschecker, J. P., & Tian, B. (2000). Mechanisms and streams for processing of "what" and "where" in auditory cortex. *Proceedings of the National Academy of Sciences, U.S.A.*, 97, 11800–11806.

Rizzolatti, G., Fadiga, L., Fogassi, L., & Gallese, V. (1997). The space around us. *Science*, 277, 190–191.

Rizzolatti, G., Scandolara, C., Matelli, M., & Gentilucci, M. (1981). Afferent properties of periarcuate neurons in macaque monkeys. II. Visual responses. *Behavioural Brain Research*, 2, 147–163.

Rodgers, K. M., Benison, A. M., Klein, A., & Barth, D. S. (2008). Auditory, somatosensory, and multisensory insular cortex in the rat. *Cerebral Cortex*, 18, 2941–2951.

Rohe, T., & Noppeney, U. (2015). Cortical hierarchies perform Bayesian causal inference in multisensory perception. *PLoS Biology*, 13, e1002073.

Rohe, T., & Noppeney, U. (2016). Distinct computational principles govern multisensory integration in primary sensory and association cortices. *Current Biology*, 26, 509–514.

Rokni, U., Richardson, A. G., Bizzi, E., & Seung, H. S. (2007). Motor learning with unstable neural representations. *Neuron*, 54, 653–666.

Romanski, L. M., Tian, B., Fritz, J., Mishkin, M., Goldman-Rakic, P. S., & Rauschecker, J. P. (1999). Dual streams of auditory afferents target multiple domains in the primate prefrontal cortex. *Nature Neuroscience*, 2, 1131–1136.

Saito, D. N., Yoshimura, K., Kochiyama, T., Okada, T., Honda, M., & Sadato, N. (2005). Cross-modal binding and

activated attentional networks during audiovisual speech integration: A functional MRI study. *Cerebral Cortex*, *15*, 1750–1760.

Salomon, R., Noel, J. P., Lukowska, M., Faivre, N., Metzinger, T., Serino, A., et al. (2017). Unconscious integration of multisensory bodily inputs in the peripersonal space shapes bodily self-consciousness. *Cognition*, *166*, 174–183.

Salomon, R., Ronchi, R., Donz, J., Bello-Ruiz, J., Herbelin, B., Martet, R., et al. (2016). The insula mediates access to awareness of visual stimuli presented synchronously to the heartbeat. *Journal of Neuroscience*, *36*, 5115–5127.

Sambo, C. F., & Foster, B. (2009). An ERP investigation on visuotactile interactions in peripersonal and extrapersonal space: Evidence for the spatial rule. *Journal of Cognitive Neuroscience*, *21*, 1550–1559.

Schmolesky, M. T., Wang, Y., Hanes, D. P., Thompson, K. G., Leutgeb, S., Schall, J. D., et al. (1998). Signal timing across the macaque visual system. *Journal of Neurophysiology*, *79*, 3272–3278.

Serino, A. (2016). Variability in multisensory responses predicts the self-space. *Trends in Cognitive Sciences*, *20*, 169–170.

Serino, A., Canzoneri, E., & Avenanti, A. (2011). Fronto-parietal areas necessary for a multisensory representation of peripersonal space in humans: An rTMS study. *Journal of Cognitive Neuroscience*, *23*, 2956–2967.

Serino, A., Noel, J. P., Galli, G., Canzoneri, E., Marmaroli, P., Lissek, H., et al. (2015). Body part-centered and full body-centered peripersonal space representations. *Scientific Reports*, *5*, 18603.

Serino, A., Noel, J.-P., Mange, R., Canzoneri, E., Pellencin, E., Bello-Ruiz, J., et al. (2017). Peripersonal space: An index of multisensory body-interaction in real, virtual, and mixed realities. *Frontiers in ICT*, *4*, 31.

Seth, A. K. (2013). Interoceptive inference, emotion, and the embodied self. *Trends in Cognitive Sciences*, *17*, 565–573.

Simon, D. M., Noel, J. P., & Wallace, M. T. (2017). Event related potentials index rapid recalibration to audiovisual temporal asynchrony. *Frontiers in Integrative Neuroscience*, *11*, 8.

Spence, C., Pavani, F., & Driver, J. (2004). Spatial constraints on visual-tactile cross-modal distractor congruency effects. *Cognitive, Affective, & Behavioral Neuroscience*, *4*, 148–169.

Spence, C., Pavani, F., Maravita, A., & Holmes, N. (2004). Multisensory contributions to the 3-D representation of visuotactile peripersonal space in humans: Evidence from the crossmodal congruency task. *Journal of Physiology-Paris*, *98*, 171–189.

Talairach, J., & Tournoux, P. (1988). *Co-planar stereotaxic atlas of the human brain: 3-Dimensional proportional system: An approach to cerebral imaging*. New York: Thieme.

Teramoto, W., Honda, K., Furuta, K., & Sekiyama, K. (2017). Visuotactile interaction even in far sagittal space in older adults with decreased gait and balance functions. *Experimental Brain Research*, *235*, 2391.

Thelen, A., Cappe, C., & Murray, M. M. (2012). Electrical neuroimaging of memory discrimination based on single-trial multisensory learning. *Neuroimage*, *62*, 1478–1488.

Valdés-Conroy, B., Sebastián, M., Hinojosa, J. A., Román, F. J., & Santaniello, G. (2014). A close look into the near/far space division: A real-distance ERP study. *Neuropsychologia*, *59*, 27–34.

Van der Stoep, N., Nijboer, T. C. W., Van der Stigchel, S., & Spence, C. (2015). Multisensory interactions in the depth plane in front and rear space: A review. *Neuropsychologia*, *70*, 335–349.

Van der Stoep, N., Serino, A., Farnè, A., Di Luca, M., & Spence, C. (2016). Depth: The forgotten dimension in multisensory research. *Multisensory Research*, *29*, 493–524.

Van der Stoep, N., Van der Stigchel, S., Nijboer, T. C. W., & Van der Smagt, M. J. (2016). Audiovisual integration in near and far space: Effects of changes in distance and stimulus effectiveness. *Experimental Brain Research*, *234*, 1175–1188.

Van der Wyk, B. C. V., Ramsay, G. J., Hudac, C. M., Jones, W., Lin, D., Klin, A., et al. (2010). Cortical integration of audio–visual speech and non-speech stimuli. *Brain and Cognition*, *74*, 97–106.

Werner, S., & Noppeney, U. (2010). Distinct functional contributions of primary sensory and association areas to audiovisual integration in object categorization. *Journal of Neuroscience*, *30*, 2662–2675.

Zampini, M., Torresan, D., Spence, C., & Murray, M. M. (2007). Auditory-somatosensory multisensory interactions in front and rear space. *Neuropsychologia*, *45*, 1869–1877.